

$O(K)$ -Approximation Coflow Scheduling in K -Core Optical Circuit Switching Networks

Xin Wang^a, Hong Shen^a, Hui Tian^b, Ye Tao^a

^aSchool of Engineering and Technology, Central Queensland University, Australia

^bSchool of Information and Communication Technology, Griffith University, Australia

Abstract—Coflow has emerged as a fundamental application-layer abstraction in distributed systems, representing communication dependencies and enabling collaborative management of related flows to enhance job completion efficiency. To meet the increasing bandwidth demands of modern data center networks (DCNs), optical circuit switches are widely deployed due to their high capacity and energy efficiency. Simultaneously, DCN deployments are evolving towards heterogeneous parallel architectures, where multiple independent optical circuit switching (OCS) cores operate concurrently to facilitate bandwidth expansion and incremental upgrades. However, existing research on coflow scheduling in multi-core switching fabrics primarily focuses on electrical packet switching (EPS) networks, with a few known results on OCS networks without or with a poor performance guarantee.

This paper studies the coflow scheduling problem in multi-core OCS networks under the *not-all-stop* (i.e., asynchronous) reconfiguration model, focusing on two major challenges of overcoming cross-core coupling for inter-core traffic allocation and satisfying the constraints of port exclusivity and reconfiguration overhead for intra-core circuit scheduling. To minimize total weighted coflow completion time (CCT), we propose an efficient algorithm by integrating linear programming-guided (LP-guided) global coflow ordering, inter-core flow allocation and intra-core circuit scheduling that achieves approximation ratios of $8K$ and $(8K + 1)$ for zero and arbitrary release times of coflows, respectively, where K is the number of OCS cores. It significantly improves the known result of $O\left(M \frac{w_{\max}}{w_{\min}} K\right)$ -approximation, where w_{\max} and w_{\min} are the maximum and minimum weights of M input coflows, respectively. This framework is also applicable to H -core EPS networks, providing approximation guarantees of $4H$ and $(4H + 1)$ for zero-time and arbitrary-time release, respectively. Trace-driven experiments using a real Facebook workload further show that the proposed algorithm delivers strong practical performance in both total weighted CCT and tail CCT.

I. INTRODUCTION

Distributed computing frameworks, such as MapReduce [1], Spark [2] and Dryad [3], structure jobs as interdependent communication stages separated by synchronization barriers. Each subsequent computation stage begins only after all parallel flows in the current stage have completed. To aggregate semantically related flows into a unified scheduling entity, the *coflow* abstraction [4] has been introduced, enabling collaborative optimization. For instance, during the MapReduce shuffle stage, each reduce worker must receive all intermediate outputs from all map workers before continuing execution. Conse-

quently, the completion of the shuffle phase is determined by the slowest individual flow, indicating that optimizing only flow completion time (FCT) is insufficient to improve job-level performance. Instead, the focus should shift to coflow completion time (CCT), defined as the completion time of the last flow within a coflow, as it more directly determines end-to-end application efficiency.

Prior research [5]–[16] on coflow scheduling has predominantly utilized the single-core electrical packet switching (EPS) model. In this model, the data center network (DCN) is abstracted as a single non-blocking switching fabric with full bisection bandwidth, simplifying the characterization of port-capacity constraints and facilitating scheduler design. Nevertheless, with the increasing traffic demands of modern data centers, EPS-based architectures encounter significant challenges related to scalability, deployment costs, and power consumption. To mitigate these issues, optical circuit switches have been incorporated into single-core DCN architectures, enabling dedicated high-capacity circuits for large-volume data transmission, thereby improving communication efficiency. Several coflow scheduling schemes [17]–[21] have been proposed within the single-core optical circuit switching (OCS) model. In addition to pure packet-switched and circuit-switched designs, recent research has extended the single-core model to hybrid EPS-OCS architectures, where packet and circuit resources coexist and are jointly optimized for coflow scheduling [22]–[25].

The traditional single-core abstraction is increasingly inadequate for representing modern data center architectures. Industry reports [26], [27] demonstrate that modern DCN architectures are evolving toward parallel designs, where multiple heterogeneous network cores operate concurrently to enhance aggregate bandwidth. In practical deployments, different generations of network architectures are often preserved and integrated rather than completely replaced, forming heterogeneous parallel networks (HPNs), in which multiple independent cores share the same set of hosts [28]. In response to this architectural evolution, previous research has investigated coflow scheduling in multi-core EPS networks, leveraging parallel packet-switched fabrics to increase network capacity [28], [29]. Parallelism is also becoming increasingly prevalent in circuit-switched fabrics. For example, Google’s Jupiter architecture replaces the traditional spine layer with a

datacenter interconnect layer composed of multiple parallel OCS cores, forming a directly connected architecture that supports flexible, data center-scale capacity upgrades and re-configurations [30]. Although such multi-core OCS infrastructures have been deployed, the corresponding coflow scheduling mechanisms remain insufficiently studied. Such architectures enable greater flexibility in capacity scaling and fundamentally alters the scheduling model.

Coflow scheduling in multi-core OCS networks faces numerous challenges. Unlike packet-switched networks, OCS-based systems are subject to two main constraints. First, port exclusivity restricts each ingress or egress port to participating in only one circuit at any given time. Second, each circuit reconfiguration incurs a non-negligible delay δ , typically ranging from hundreds of microseconds to milliseconds. Existing OCS reconfiguration mechanisms are generally divided into the *all-stop* and *not-all-stop* models (see Subsection III-C). In the *all-stop* (i.e., synchronous) model, whenever the circuit configuration changes, all ongoing transmissions are paused. In contrast, the *not-all-stop* (i.e., asynchronous) model only interrupts the ports involved in the circuit update, while transmissions on unaffected circuits continue uninterrupted. This paper focuses on the *not-all-stop* model, which is more practically relevant but also more challenging, as it further complicates resource coupling and scheduling decisions.

When multiple OCS cores operate in parallel, coflow scheduling must jointly determine flow allocation across cores and circuit scheduling within each core, while respecting one-to-one port exclusivity and non-negligible reconfiguration overhead under the *not-all-stop* model. In contrast to single-core OCS scheduling or multi-core EPS scheduling, the combination of inter-core traffic coupling and OCS-specific switching constraints makes this problem more challenging. This study addresses the multi-coflow scheduling problem in multi-core OCS networks and introduces an approximation algorithm with a provable guarantee for minimizing the total weighted CCT. Notably, the proposed approach significantly advances the prior work [31] by establishing an $O\left(M \frac{w_{\max}}{w_{\min}} K\right)$ -approximation bound for the same multi-core OCS scenario. Additionally, the proposed framework can be naturally applied to multi-core EPS networks by setting the reconfiguration delay to zero (i.e., $\delta = 0$) and substituting the OCS-specific lower bounds with the corresponding lower bounds tailored to the EPS setting, thereby yielding approximation guarantees.

The main contributions of this paper are summarized as follows:

- We formulate the coflow scheduling problem in multi-core OCS networks under the *not-all-stop* reconfiguration model and propose an efficient algorithm that combines LP-guided global coflow ordering, inter-core flow allocation and intra-core circuit scheduling.
- We show that our algorithm achieves approximation ratios of $8K$ and $(8K + 1)$ for zero-release and arbitrary-release times of coflows, respectively, in a K -core OCS

network, enabling a performance guarantee based solely on the architectural layout of the switching fabric rather than on input features. It represents a significant improvement over the known result, which has an approximation ratio proportional to the product of the coflow max-to-min weight ratio $\frac{w_{\max}}{w_{\min}}$, the number of coflows M and K .

- We demonstrate that the proposed algorithm framework can be naturally applied to multi-core EPS networks. Specifically, for an H -core EPS network, the algorithm achieves approximation ratios of $4H$ and $(4H + 1)$ under zero-release and arbitrary-release settings, respectively, thus providing a unified approximation perspective for multi-core OCS and EPS architectures.
- We conduct extensive trace-driven simulations using real Facebook workloads to evaluate the proposed algorithm. The results demonstrate that the algorithm achieves superior overall performance, consistently outperforming representative ablation baselines and significantly reducing both total weighted CCT and tail CCT, thereby validating its practical effectiveness.

The remainder of this paper is organized as follows: Section II reviews related research and provides a comparative analysis; Section III introduces the system model and formal problem formulation; Section IV describes the proposed multiple coflow scheduling algorithm and its theoretical performance guarantees; Section V presents experimental results using a realistic Facebook trace; Section VI concludes this paper.

II. RELATED WORK

Coflow scheduling has been investigated across a range of data center network (DCN) switching models. Initial research focused on the single-core electrical packet switching (EPS) model. Later studies expanded coflow scheduling to single-core optical circuit switching (OCS) scenarios, encompassing both pure OCS and hybrid EPS-OCS architectures, and considering both *all-stop* and *not-all-stop* reconfiguration mechanisms. Additionally, research has explored multi-core EPS architectures, where multiple packet-switched cores operate simultaneously to enhance aggregate bandwidth. However, coflow scheduling in multi-core OCS networks remains underexplored. This section reviews relevant literature from these perspectives and presents a comparative summary in Table I.

A. Coflow Scheduling in Single-Core EPS Networks

Orchestra [5] is widely considered the first study to introduce the coflow abstraction and demonstrate that even a simple FIFO-based strategy can significantly improve performance through coflow-aware scheduling. Varys [7] proposed two greedy heuristics: smallest-effective-bottleneck-first (SEBF) and minimum-allocation-for-desired-duration (MADD), for greedily scheduling coflows based on bottleneck completion time in single-core EPS networks, with the goal of minimizing the overall CCT. In decentralized environments, Barrat [8] used multiplexing techniques to solve the head-of-line

TABLE I: COMPARISON AMONG RELATED WORK

Works	Single-Core		Multi-Core		Provable Guarantee
	EPS-Enable	OCS-Enable	EPS-Enable	OCS-Enable	
Varys [7], Barrat [8], D-CAS [9], CODA [11]	✓	✗	✗	✗	✗
Qiu <i>et al.</i> [14], Khuller <i>et al.</i> [32], Shafiee <i>et al.</i> [15]	✓	✗	✗	✗	✓
OMCO [17]	✗	✓	✗	✗	✗
Sunflow [20], Reco-Sin [18], Reco-Mul+ [19], GOS [21]	✗	✓	✗	✗	✓
Co-scheduler [23], ONS [25]	✓	✓	✗	✗	✗
Wang <i>et al.</i> [22], Wang <i>et al.</i> [24]	✓	✓	✗	✗	✓
Weaver [28], Chen [33], Chen [29]	✗	✗	✓	✗	✓
Wang <i>et al.</i> [31], Our Work	✗	✗	✗	✓	✓

blocking problem of small coflows, while D-CAS [9] also focused on decentralized coflow scheduling. Aalo [10] and NC-DRF [34] are two well-known information-agnostic coflow schedulers that prioritize efficiency and fairness, respectively. Specifically, Aalo [10] proposed a discretized coflow-aware least-attained service (D-CLAS) algorithm that can operate efficiently without prior knowledge of flow information. In contrast, NC-DRF [34] was designed to ensure isolation using load-balancing principles. CODA [11] was the first to apply machine learning to identify coflows between individual flows. Recently, Wang *et al.* [12] proposed a multi-stage online job scheduling framework based on deep reinforcement learning (DRL). In subsequent work, Wang *et al.* [13] combined limited multiplexing with DRL to reduce the average weighted CCT while maintaining fairness. However, these methods are predominantly heuristic and lack provable worst-case performance guarantees.

At the theoretical level, several approximation results have been established. Qiu *et al.* [14] proposed a deterministic algorithm with an approximation ratio of $\frac{67}{3}$ to minimize the total weighted CCT. Khuller *et al.* [32] modeled the problem as a concurrent open-shop problem and derived a 12-approximation algorithm. Shafiee *et al.* [15] subsequently improved this bound to 5 using a linear programming (LP) approach, while Wang *et al.* [16] achieved a 2-approximation algorithm by simplifying the process and eliminating the need for LP solving. Most of these works focus on single-stage coflow scheduling without considering the dependencies between coflows within a job. Tian *et al.* [35] were the first to investigate the scheduling of dependent coflows for multi-stage jobs, establishing an approximation ratio of $(2N + 1)$, where N represents the number of hosts. Subsequently, Shafiee *et al.* [6] developed a polynomial-time algorithm with an approximation ratio of $O\left(\frac{\mu \log(N)}{\log(\log(N))}\right)$, where μ represents the maximum number of coflows in the job.

B. Coflow Scheduling in Single-Core OCS Networks

Research on coflow scheduling for single-core OCS architectures, including pure OCS and hybrid OCS-EPS architectures, remains relatively limited. Given the two main OCS reconfiguration paradigms, the *all-stop* model and the *not-all-stop* model, this paper reviews the existing literature under both settings.

1) *All-Stop Reconfiguration Model*: OMCO [17] was the first online algorithm for multi-coflow scheduling in single-core pure OCS networks. Reco-Sin [18] and Reco-Mul+ [19] established the first approximation guarantees for single-coflow and multi-coflow scheduling in a single-core pure OCS network, with approximation ratios of 2 and $8M$, respectively, where M represents the number of coflows. The above methods are based on Birkhoff-von Neumann (BvN) decomposition [36]. Furthermore, Wang *et al.* [22] developed approximation algorithms with provable performance guarantees for both single and multiple coflow scheduling in a single-core hybrid EPS-OCS network. All these methods assume that the OCS operates under the *all-stop* model.

2) *Not-All-Stop Reconfiguration Model*: Under the *not-all-stop* model, Sunflow [20] first proposed a constant-factor approximation algorithm for single-coflow scheduling in single-core pure OCS networks, and a heuristic method for scheduling multiple coflows. Subsequently, GOS [21] developed a 4-approximation algorithm for multi-coflow scheduling in a single-core pure OCS network. In a hybrid optical-electrical environment, Co-scheduler [23] first considered both optical-electrical hybrid-switching characteristics and coflow structures, although it did not provide formal performance guarantees. ONS [25] proposed an online heuristic algorithm for minimizing the total CCT in single-core hybrid EPS-OCS networks, also without theoretical performance bounds. All these methods are based on the *not-all-stop* reconfiguration model.

C. Coflow Scheduling in Multi-Core EPS Networks

In recent years, the coflow scheduling problem in multi-core EPS networks has attracted increasing attention. Weaver [28] studied single-coflow scheduling in heterogeneous parallel networks (HPNs), and proposed an $O(K)$ -approximation algorithm, where K is the number of network cores. Chen [33] further studied the multi-coflow scheduling in HPNs and derived an $O\left(\frac{\log K}{\log \log K}\right)$ -approximation algorithm. Furthermore, Chen [29] considered identical parallel networks and developed coflow-level approximation algorithms with approximation ratios of $4K + 1$ and $4K$ for arbitrary and zero release times, respectively, where K represents the number of identical cores.

D. Coflow Scheduling in Multi-Core OCS Networks

Previous studies have examined the coflow scheduling problem in single-core EPS and OCS architectures, as well as in multi-core EPS networks. However, theoretical advancements in multi-core OCS environments remain limited. To the best of our knowledge, Wang *et al.* [31] were the first to analyze multi-coflow scheduling in multi-core OCS networks, establishing an $O\left(M \frac{w_{\max}}{w_{\min}} K\right)$ -approximation guarantee, where M is the number of coflows, K denotes the number of OCS cores, and w_{\max} and w_{\min} are the maximum and minimum coflow weights, respectively. Consequently, the approximation ratio is influenced by both the network size and input-dependent parameters, including the number of coflows and the weight range. In contrast, this work introduces a provable approximation algorithm for multi-coflow scheduling in a K -core OCS network under the *not-all-stop* (asynchronous) reconfiguration model, achieving an $O(K)$ -approximation guarantee that depends solely on the architectural parameter K . This result represents a substantial improvement over the previously established bound for the same setting.

III. SYSTEM MODEL AND PROBLEM FORMULATION

This section introduces the system model, including the network architecture, traffic abstraction, and optical circuit switching (OCS) reconfiguration mechanism. Based on this model, the multi-coflow scheduling problem in heterogeneous parallel networks (HPNs) is formally defined, and its computational complexity is analyzed. The main symbols used in this paper are summarized in Table II.

A. Network Architecture

This paper considers an HPN composed of K independent, non-blocking OCS cores operating in parallel, as illustrated in Fig. 1. The index set of OCS cores is denoted by $\mathcal{K} = \{1, \dots, K\}$, where each core $k \in \mathcal{K}$ corresponds to one OCS. The index sets of source and destination servers are denoted by \mathcal{I} and \mathcal{J} , respectively, with $|\mathcal{I}| = |\mathcal{J}| = N$. The network interconnects N source servers $\{s_i : i \in \mathcal{I}\}$ and N destination servers $\{d_j : j \in \mathcal{J}\}$. Accordingly, each core forms an independent, non-blocking $N \times N$ switching fabric.

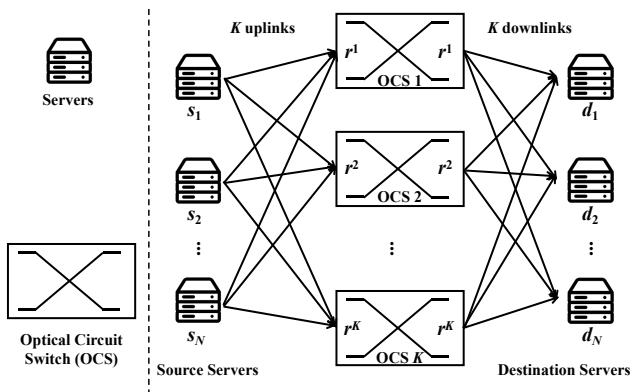


Fig. 1: Heterogeneous Multi-Core DCN Architecture

TABLE II: Mathematical Symbols

Symbol	Definition
\mathcal{C}	The set of coflows
\mathcal{M}	The index set of coflows
M	The number of coflows, i.e., $M = \mathcal{M} $
\mathcal{K}	The index set of parallel OCS cores
K	The number of OCS cores, i.e., $K = \mathcal{K} $
N	The number of ingress/egress ports per core
\mathcal{I}, \mathcal{J}	The index sets of source servers and destination servers, i.e., $ \mathcal{I} = \mathcal{J} = N$
p	Any port in $\mathcal{I} \cup \mathcal{J}$
C_m	The m -th coflow, where $1 \leq m \leq M$
\mathcal{F}_m	The set of flows in C_m
D_m	The demand matrix of C_m
D_m^k	The portion of D_m allocated to core k
$f_m(i, j)$	The flow from ingress port i to egress port j of C_m
$f_m^k(i, j)$	The subflow of $f_m(i, j)$ transmitted on core k
$t_m^k(i, j)$	The circuit establishment time of $f_m^k(i, j)$ on core k
$d_m(i, j) / d_m^k(i, j)$	The data size of $f_m(i, j) / f_m^k(i, j)$
$\rho_{m,p} / \rho_{m,p}^k$	The load incident to port p in D_m / D_m^k
$\tau_{m,p} / \tau_{m,p}^k$	The number of nonzero entries incident to port p in D_m / D_m^k
ρ_m / ρ_m^k	The maximum port load in D_m / D_m^k
τ_m / τ_m^k	The maximum number of nonzero entries in D_m / D_m^k
$D_{1:m}$	The prefix-aggregated demand matrix of first m coflows, i.e., $D_{1:m} = \sum_{\ell=1}^m D_\ell$
$D_{1:m}^k$	The prefix-aggregated demand matrix on core k for the first m coflows i.e., $D_{1:m}^k = \sum_{\ell=1}^m D_\ell^k$
$\rho_{1:m,p} / \rho_{1:m,p}^k$	The aggregate load incident to port p in $D_{1:m} / D_{1:m}^k$
$\tau_{1:m,p} / \tau_{1:m,p}^k$	The number of nonzero entries incident to port p in $D_{1:m} / D_{1:m}^k$
$\rho_{1:m} / \rho_{1:m}^k$	The maximum aggregate load in $D_{1:m} / D_{1:m}^k$
$\tau_{1:m} / \tau_{1:m}^k$	The maximum number of nonzero entries in $D_{1:m} / D_{1:m}^k$
r^k	The per-port transmission rate of core k
R	The aggregated port transmission rate across all cores, i.e., $R = \sum_{k \in \mathcal{K}} r^k$
w_m	The weight of C_m
a_m	The release time of C_m
δ	The reconfiguration delay
T_m^k	The completion time of the portion of coflow C_m allocated to core k
T_m	The completion time of coflow C_m

Each source server is equipped with K parallel uplinks, each of which connects to a different OCS core; each destination server has K corresponding downlinks. In core k , source server s_i is connected to ingress port i , and destination server d_j is connected to egress port j , where $i \in \mathcal{I}$ and $j \in \mathcal{J}$. Each core $k \in \mathcal{K}$ operates independently at a per-port transmission rate r^k , capturing the heterogeneity in link capacities across cores. Therefore, traffic can be allocated across multiple cores, while circuit scheduling is performed independently within each core. Let $R = \sum_{k \in \mathcal{K}} r^k$ represent the aggregated port transmission rate across all cores.

B. Traffic Abstraction

We utilize the *coflow* abstraction [4] to model application-level communication requirements in HPNs. A coflow contains a set of parallel flows that must be completed jointly to realize

a single communication stage of an application across multiple machines.

Let $\mathcal{C} \triangleq \{C_m : m \in \mathcal{M}\}$ be the set of coflows, where $\mathcal{M} = \{1, \dots, M\}$ is the index set of coflows. Each coflow C_m contains a set of flows \mathcal{F}_m . For each $m \in \mathcal{M}$ and port pair $(i, j) \in \mathcal{I} \times \mathcal{J}$, the flow $f_m(i, j) \in \mathcal{F}_m$ represents traffic from source server s_i (equivalently, ingress port i) to destination server d_j (equivalently, egress port j) with data size $d_m(i, j)$. Accordingly, each coflow C_m is characterized by a demand matrix $D_m = [d_m(i, j)]_{i \in \mathcal{I}, j \in \mathcal{J}}$ of dimension $|\mathcal{I}| \times |\mathcal{J}|$ (i.e., $N \times N$).

C. Reconfiguration Mechanism

Due to the circuit-switching nature of OCS, each core k establishes a one-to-one matching between its ingress and egress ports at any given time. A circuit configuration can be represented as a matching in the bipartite graph induced by the ingress and egress ports, ensuring that each port participates in at most one active circuit. Each circuit reconfiguration incurs a fixed delay δ . During reconfiguration, the affected ports are unavailable for data transmission.

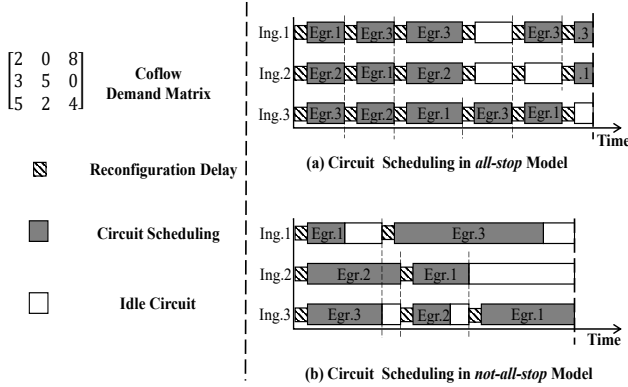


Fig. 2: Circuit Reconfiguration Models in an OCS Core

The circuit configurations evolve according to two standard reconfiguration models, namely the *all-stop* or *not-all-stop* models, as shown in Fig. 2. In the *all-stop* model (Fig. 2(a)), reconfiguration is synchronous: whenever the configuration changes, all ongoing transmissions are paused. This model is conceptually simple and is often associated with preemptive scheduling. However, such global suspension may lead to unnecessary port idleness and reduced resource utilization. In contrast, the *not-all-stop* model (Fig. 2(b)) adopts asynchronous reconfiguration, in which only the ports involved in the circuit update are interrupted, while other established circuits continue transmitting. In this setting, once a flow begins transmission on a circuit, the transmission is typically non-preemptive. Although this model improves link utilization and reduces unnecessary interruptions, it also increases scheduling complexity due to asynchronous reconfiguration.

D. Problem Definition

Consider a set of coflows \mathcal{C} , where each coflow $C_m \in \mathcal{C}$ is associated with a demand matrix $D_m = [d_m(i, j)]_{i \in \mathcal{I}, j \in \mathcal{J}}$,

a positive weight w_m , and a release time $a_m \geq 0$. The goal is to schedule all flows $f_m(i, j)$ on a K -core OCS network under the asynchronous (*not-all-stop*) reconfiguration model. A feasible schedule includes the following components:

- *Global Coflow Ordering*: A permutation of $\mathcal{M} = \{1, \dots, M\}$ that specifies the global priority order of coflows. During execution, this order is enforced among coflows that have already been released.
- *Inter-Core Flow Allocation*: For each coflow C_m with demand matrix D_m , determine an allocation $\{D_m^k\}_{k \in \mathcal{K}}$, where $k \in \mathcal{K}$ such that $D_m = \sum_{k \in \mathcal{K}} D_m^k$. Here, $D_m^k = [d_m^k(i, j)]_{i \in \mathcal{I}, j \in \mathcal{J}}$ denotes the portion of D_m allocated to core k , satisfying $d_m^k(i, j) \geq 0$ and $\sum_{k \in \mathcal{K}} d_m^k(i, j) = d_m(i, j)$, $\forall (i, j) \in \mathcal{I} \times \mathcal{J}$.
- *Intra-Core Circuit Scheduling*: For each core $k \in \mathcal{K}$ and each subflow $f_m^k(i, j)$ with $d_m^k(i, j) > 0$, determine a circuit schedule $S_m^k = \{i, j, t_m^k(i, j)\}$, where $t_m^k(i, j)$ represents the circuit establishment time of $f_m^k(i, j)$. Each subflow can be scheduled only after the release time of its coflow, i.e., $t_m^k(i, j) \geq a_m$, since coflow C_m is unavailable before time a_m .

Under the *not-all-stop* model, the transmission of subflow $f_m^k(i, j)$ starts from $t_m^k(i, j) + \delta$ and completes at $T_m^k(i, j) = t_m^k(i, j) + \delta + \frac{d_m^k(i, j)}{r^k}$. The completion time of the portion of coflow C_m assigned to core k is defined as $T_m^k = \max_{(i, j) \in \mathcal{I} \times \mathcal{J}} T_m^k(i, j)$, and the overall coflow completion time (CCT) is $T_m = \max_{k \in \mathcal{K}} T_m^k$. The goal is to minimize the total weighted CCT: $\min \sum_{m \in \mathcal{M}} w_m T_m$.

E. Hardness Analysis

When the reconfiguration delay δ is infinity, i.e., $\delta = \infty$, the scheduling problem for a single coflow in a single-core OCS network reduces to a non-preemptive open-shop scheduling problem with the objective of minimizing the makespan, which is *NP-hard* [37]. Furthermore, even in two-port OCS networks, the single-coflow scheduling problem remains *NP-hard* for any finite reconfiguration delay where $0 < \delta < \infty$ [20].

The multi-core OCS scheduling problem considered in this paper is a strict generalization of the single-core case. Specifically, any instance on a single-core OCS network can be represented as a K -core network by allocating all traffic to one core and leaving the remaining cores idle. Therefore, the single-coflow scheduling problem in a multi-core OCS network is also *NP-hard*. Consequently, the multi-coflow problem is *NP-hard* as well, since the single-coflow case is a special case corresponding to $M = 1$.

IV. MULTI-CORE COFLOW SCHEDULING

This section presents an approximation algorithm (Algorithm 1) for multi-coflow scheduling in heterogeneous multi-core OCS networks under the *not-all-stop* reconfiguration model, and establishes its provable performance guarantees. The proposed method consists of three main components: (i) LP-guided global coflow ordering, (ii) inter-core flow allocation, and (iii) intra-core circuit scheduling.

To support algorithm design, we derive a local single-core lower bound associated with a given inter-core flow allocation, which characterizes the minimum completion time requirement on a single core. To support the approximation analysis, we then construct a prefix-aware global lower bound via an ordering-based linear programming (LP) relaxation, which characterizes the overall scheduling performance.

A. Derivation of the Lower Bounds

Consider a coflow C_m with demand matrix $D_m = [d_m(i, j)]_{i \in \mathcal{I}, j \in \mathcal{J}}$. For any port $p \in \mathcal{I} \cup \mathcal{J}$, the aggregate traffic load incident to port p is defined as

$$\rho_{m,p} \triangleq \begin{cases} \sum_{j \in \mathcal{J}} d_m(i, j), & \text{if } p = i \in \mathcal{I}, \\ \sum_{i \in \mathcal{I}} d_m(i, j), & \text{if } p = j \in \mathcal{J}, \end{cases}$$

and the corresponding reconfiguration count, i.e., the number of nonzero entries incident to port p , is defined as

$$\tau_{m,p} \triangleq \begin{cases} \sum_{j \in \mathcal{J}} \mathbf{1}[d_m(i, j) > 0], & \text{if } p = i \in \mathcal{I}, \\ \sum_{i \in \mathcal{I}} \mathbf{1}[d_m(i, j) > 0], & \text{if } p = j \in \mathcal{J}. \end{cases}$$

The maximum port load in D_m is defined as $\rho_m \triangleq \max_{p \in \mathcal{I} \cup \mathcal{J}} \rho_{m,p}$, and the maximum number of nonzero entries in D_m is defined as $\tau_m \triangleq \max_{p \in \mathcal{I} \cup \mathcal{J}} \tau_{m,p}$. In a K -core OCS network, let r^k represent the per-port transmission rate of core k , and let $R = \sum_{k \in \mathcal{K}} r^k$ denote the aggregate port rate across all cores.

1) *Single-Core Lower Bound*: Consider any allocation $\{D_m^k\}_{k \in \mathcal{K}}$ such that $D_m = \sum_{k \in \mathcal{K}} D_m^k$, where $D_m^k = [d_m^k(i, j)]_{i \in \mathcal{I}, j \in \mathcal{J}}$ denotes the portion of D_m allocated to core k . For each core $k \in \mathcal{K}$ and each port $p \in \mathcal{I} \cup \mathcal{J}$, the incident traffic load and reconfiguration count on core k are defined as

$$\rho_{m,p}^k \triangleq \begin{cases} \sum_{j \in \mathcal{J}} d_m^k(i, j), & \text{if } p = i \in \mathcal{I}, \\ \sum_{i \in \mathcal{I}} d_m^k(i, j), & \text{if } p = j \in \mathcal{J}, \end{cases}$$

and

$$\tau_{m,p}^k \triangleq \begin{cases} \sum_{j \in \mathcal{J}} \mathbf{1}[d_m^k(i, j) > 0], & \text{if } p = i \in \mathcal{I}, \\ \sum_{i \in \mathcal{I}} \mathbf{1}[d_m^k(i, j) > 0], & \text{if } p = j \in \mathcal{J}. \end{cases}$$

The maximum port load of D_m^k is defined as $\rho_m^k \triangleq \max_{p \in \mathcal{I} \cup \mathcal{J}} \rho_{m,p}^k$, and the maximum number of nonzero entries in D_m^k is defined as $\tau_m^k \triangleq \max_{p \in \mathcal{I} \cup \mathcal{J}} \tau_{m,p}^k$. For a given allocation $\{D_m^k\}_{k \in \mathcal{K}}$, let $T_{\text{LB}}^k(\cdot)$ denote the CCT lower bound of the traffic allocated to core k .

Since each port can only participate in one circuit at a time, transmitting the total load incident to port p on core k requires at least $\rho_{m,p}^k / r^k$. In addition, each nonzero flow incident to that port requires one circuit establishment, leading to a total reconfiguration delay of at least $\tau_{m,p}^k \delta$. Taking the maximum over all ports yields the lower bound. For any nonzero demand matrix $D_m^k \neq \mathbf{0}_{|\mathcal{I}| \times |\mathcal{J}|}$, the single-core lower bound is given by

$$T_{\text{LB}}^k(D_m^k) \triangleq \max_{p \in \mathcal{I} \cup \mathcal{J}} L_{m,p}^k, \quad (1)$$

where $L_{m,p}^k = \frac{\rho_{m,p}^k}{r^k} + \tau_{m,p}^k \delta$.

Lemma 1 (Single-Core Lower Bound). *In a K -core OCS network, for any nonzero assigned demand matrix $D_m^k \neq \mathbf{0}_{|\mathcal{I}| \times |\mathcal{J}|}$, the completion time of the portion of coflow C_m assigned to core k satisfies $T_m^k \geq \max_{p \in \mathcal{I} \cup \mathcal{J}} \left(\frac{\rho_{m,p}^k}{r^k} + \tau_{m,p}^k \delta \right)$.*

The lower bound $T_{\text{LB}}^k(D_m^k)$ depends on the specific flow allocation $\{D_m^k\}_{k \in \mathcal{K}}$ and is therefore allocation-dependent. To derive an approximation ratio relative to the optimal schedule, we need a global lower bound that depends only on the original demand matrix D_m and network parameters, rather than on any particular allocation or schedule.

Prior work [31] established the allocation-independent single-coflow lower bound $T_{\text{LB}}(D_m) \triangleq \delta + \frac{\rho_m}{R}$. However, this bound applies only to a single coflow and does not capture prefix interactions among multiple coflows, which are crucial for analyzing the total weighted CCT. As a result, relying on this bound alone may lead to an approximation factor that scales with the number of coflows M . To overcome this limitation, we next develop a prefix-aware global lower bound via an ordering-based LP relaxation, which explicitly captures the cumulative transmission and reconfiguration workloads induced by preceding coflows.

2) *Prefix-Aware Lower Bound*: Inspired by the classical ordering-based LP relaxation framework, which has been widely used in multi-coflow scheduling for single-core EPS networks [15], we formulate the following LP relaxation for the multi-core OCS scheduling problem.

To capture the aggregate service capability of the multi-core OCS network, we adopt an aggregated resource view for each source or destination port $p \in \mathcal{I} \cup \mathcal{J}$. Under this view, traffic can be processed in parallel across K cores, where each core k provides a per-port transmission rate r^k . Therefore, the *aggregate transmission rate* available for port p across all cores is $\sum_{k \in \mathcal{K}} r^k (= R)$. Furthermore, since each port p independently participates in circuit reconfiguration operations across different cores, and each such operation on each core requires δ time units, each core contributes a reconfiguration-processing rate of at most $1/\delta$. Hence, the *aggregate reconfiguration-processing rate* associated with port p across all cores is at most K/δ .

The LP formulation introduces a relaxed ordering variable $x_{m,m'} \in [0, 1]$, which represents the completion precedence relation between coflows C_m and $C_{m'}$. The ordering variables satisfy the constraint, i.e.,

$$x_{m,m'} + x_{m',m} = 1, \forall m \neq m'. \quad (2)$$

In an exact integer programming (IP) formulation, $x_{m,m'} \in \{0, 1\}$, where $x_{m,m'} = 1$ indicates that coflow C_m completes before coflow $C_{m'}$ and $x_{m,m'} = 0$ otherwise. In the LP relaxation, $x_{m,m'}$ is allowed to take any value in $[0, 1]$, i.e.,

$$0 \leq x_{m,m'} \leq 1, \forall m \neq m'. \quad (3)$$

From the aggregated resource perspective, the formulation imposes two necessary capacity constraints for each coflow C_m and each port $p \in \mathcal{I} \cup \mathcal{J}$:

(i) **Transmission-Capacity Constraints:** By the time coflow C_m completes, all coflows ordered before C_m , together with C_m itself, must have already transmitted all traffic incident to port p . Since the available aggregate transmission rate available on port p is R , the cumulative transmitted load by time T_m cannot exceed RT_m . Hence,

$$T_m \geq \frac{1}{R} \left(\rho_{m,p} + \sum_{m' \neq m} \rho_{m',p} x_{m',m} \right), \forall m, p. \quad (4)$$

(ii) **Reconfiguration-Capacity Constraints:** Similarly, when coflow C_m completes, all reconfiguration operations associated with coflows ordered before C_m , together with those required by C_m , must also have been completed on port p . Since the aggregate reconfiguration-processing rate available on port p is upper bounded by K/δ , the cumulative number of such reconfiguration operations cannot exceed $(K/\delta)T_m$. Therefore,

$$T_m \geq \frac{\delta}{K} \left(\tau_{m,p} + \sum_{m' \neq m} \tau_{m',p} x_{m',m} \right), \forall m, p. \quad (5)$$

In addition, since coflow C_m cannot complete before it is released, we impose the release-time constraints

$$T_m \geq a_m, \forall m. \quad (6)$$

Collecting the above constraints, we obtain the following LP relaxation:

$$\min \sum_{m \in \mathcal{M}} w_m T_m, \quad \text{s.t. (2) - (6)}.$$

Let $(\tilde{T}_m, \tilde{x}_{m,m'})$ denote the optimal solution to the LP relaxation, and let T_m^* denote the completion time of coflow C_m in an optimal feasible schedule to the original problem. Since any feasible schedule for the original problem induces a feasible integral solution to the LP, the formulation is a valid relaxation of the original scheduling problem. Consequently, the objective value of the LP relaxation provides a valid lower bound on the optimal value of the original problem, namely $\sum_{m=1}^M w_m \tilde{T}_m \leq \sum_{m=1}^M w_m T_m^*$.

B. Approximation Algorithm

Our algorithm framework adopts an LP-guided combinatorial construction, rather than a standard LP-rounding paradigm. The LP relaxation plays two roles: (i) its objective value provides the lower bound used in the approximation analysis, and (ii) its completion values $\{\tilde{T}_m\}_{m \in \mathcal{M}}$ serve as surrogate priority indicators for constructing the global coflow ordering. Importantly, the feasible scheduling scheme is not obtained by rounding in the LP solution; instead, the final feasible scheduling scheme (including flow allocation and circuit scheduling) is directly generated by a greedy combinatorial procedure. The

core of the analysis is then to prove that the objective value of the constructed feasible schedule is at most a constant-factor multiple of the objective value of the LP relaxation, thereby establishing the approximation ratio of our algorithm.

Consistent with the intuitive three-stage framework adopted in [31], Algorithm 1 consists of three components: (i) global coflow ordering, (ii) inter-core flow allocation, and (iii) intra-core circuit scheduling. The key difference in our approach lies in the LP-guided global ordering and the corresponding approximation analysis.

1) *LP-guided Global Coflow Ordering:* We first solve the ordering-based LP relaxation introduced in Subsection IV-A2. Let \tilde{T}_m denote the value of the LP variable T_m associated with coflow C_m in the LP solution, which serves as a lower bound on its completion time in the original scheduling problem. The coflows are then sorted in non-decreasing order of \tilde{T}_m , and re-indexed accordingly so that $\tilde{T}_1 \leq \tilde{T}_2 \leq \dots \leq \tilde{T}_M$, with ties broken arbitrarily. This LP-guided order is adopted as the global coflow priority order throughout the algorithm. During scheduling, this order is enforced among released coflows. Unless otherwise specified, all subsequent coflow indices refer to this reordered sequence.

2) *Inter-Core Flow Allocation:* The inter-core flow allocation is a prefix-aware greedy assignment procedure. Coflows are processed sequentially according to the re-indexed order. Each flow is allocated entirely to a single core, and flow splitting is not allowed to avoid packet reordering, buffering overhead, and additional control-plane complexity in practical multi-core OCS deployments [28]. Restricting allocation to the flow level ensures both analytical tractability and practical implementability.

For each flow $f_m(i, j)$, the algorithm selects the core that minimizes the single-core prefix lower bound $T_{\text{LB}}^k(D_{1:m}^k \oplus d_m(i, j))$ after allocation. Intuitively, this rule aims to prevent any single core from becoming the dominant prefix bottleneck, thereby reducing the cumulative queuing and blocking effects that subsequent coflows may encounter on overloaded cores, and thus indirectly reducing the final weighted total CCT. The internal processing order of flows within a coflow does not affect the approximation guarantee. In practice, allocating larger flows earlier may reduce their impact on the final total weighted CCT.

3) *Intra-Core Circuit Scheduling:* After the allocation phase, each core independently schedules the traffic allocated to it, while adhering to the global coflow priority order among released coflows. The intra-core circuit scheduling phase employs a greedy earliest-feasible port-matching scheduler, following a fixed global coflow order: it scans subflows according to the global coflow order and schedules the first released subflow with both its ingress and egress ports idle at the earliest feasible time. The design goal is to avoid unnecessary port idleness and maximize core utilization, thereby improving the final performance of each core. The intra-core circuit scheduling policy exhibits the following properties:

- *Port-Exclusive:* Each ingress and egress port can participate in at most one active circuit at any given time,

thus satisfying the one-to-one port matching constraint of OCS.

- *Non-Preemptive*: Once a flow begins transmission, it continues until completion without interruption, avoiding additional reconfiguration overhead.
- *Work-Conserving*: When no high-priority flows are waiting to be processed on a port pair, low-priority flows can be processed first, ensuring that no eligible port pairs remain idle.

The algorithm first determines the global coflow priority order by solving the LP relaxation of the original problem (Lines 1-2). The coflows are then sorted in non-decreasing order of \tilde{T}_m and re-indexed accordingly, so that $\tilde{T}_1 \leq \tilde{T}_2 \leq \dots \leq \tilde{T}_M$.

Subsequently, the algorithm enters the flow allocation phase (Lines 3-15). For each core $k \in \mathcal{K}$, a prefix-aggregated matrix $D_{1:m}^k = \sum_{\ell=1}^m D_\ell^k$ is maintained to represent the aggregate traffic allocated to core k from the first m coflows in the re-indexed order. For each core k , the matrix $D_{1:0}^k$ is initialized to zero (Line 3). For each coflow C_m processed sequentially (Line 4), for all $k \in \mathcal{K}$, $D_{1:m}^k$ is set to $D_{1:m-1}^k$ to ensure that each core inherits the prefix load of the first $m-1$ coflows before any flow of C_m is allocated (Line 5). The per-core allocation matrices D_m^k are also initialized to zero for all $k \in \mathcal{K}$ (Line 6). Let \mathcal{F}_m denote the set of nonzero flows in C_m (Line 7), which is then sorted in non-increasing order of $d_m(i, j)$ (Line 8). For each flow $f_m(i, j) \in \mathcal{F}_m$ (Line 9), the algorithm tentatively places it on every core k by constructing $D_{1:m}^k \oplus d_m(i, j)$, which increases the (i, j) -th entry of $D_{1:m}^k$ by $d_m(i, j)$. This operation is equivalent to $D_{1:m}^k + d_m(i, j) E_{ij}$, where $E_{ij} \in \mathbb{R}^{N \times N}$ is the standard basis matrix with a 1 in entry (i, j) and zeros elsewhere. The core k^* is then selected as $k^* \leftarrow \operatorname{argmin}_{k \in \mathcal{K}} T_{\text{LB}}^k(D_{1:m}^k \oplus d_m(i, j))$ (Line 10), corresponding to the core that yields the minimum single-core lower bound after adding this flow. The entire flow is allocated to core k^* (Line 11), and both $D_m^{k^*}$ and $D_{1:m}^{k^*}$ are updated accordingly (Lines 12-13). After all flows in C_m have been allocated, the matrices $\{D_m^k\}_{k \in \mathcal{K}}$ represent its inter-core allocation, and $\{D_{1:m}^k\}_{k \in \mathcal{K}}$ are carried forward to the next iteration.

In the final phase, intra-core circuit scheduling is performed independently on each core (Lines 16-30). For each core $k \in \mathcal{K}$, the circuit schedule S_m^k for each coflow $m \in \mathcal{M}$ is initialized (Lines 17-19). The set $\mathcal{F}^k \triangleq \bigcup_{m \in \mathcal{M}} \{f_m^k(i, j) \mid d_m^k(i, j) > 0\}$ is constructed, containing all unfinished subflows allocated to core k (Line 20). Scheduling decisions are made over the released subflows in \mathcal{F}^k according to the re-indexed global coflow priority order. While \mathcal{F}^k is non-empty (Line 21), the scheduler scans the subflows in \mathcal{F}^k in that order (Line 22), and sequentially selects the first released subflow $f_m^k(i, j)$ whose ingress port i and egress port j are both idle (Line 23). The selected subflow is then scheduled at the earliest feasible circuit establishment time $t_m^k(i, j)$, which is no earlier than the release time a_m of its coflow and is constrained by the availability of ports i and j . Its

Algorithm 1 Multi-Coflow Scheduling in Multi-Core OCS Networks

Input: demand matrices $\{D_m = [d_m(i, j)]\}_{m \in \mathcal{M}}$; weights $\{w_m\}_{m \in \mathcal{M}}$; release times $\{a_m\}_{m \in \mathcal{M}}$; core rates $\{r^k\}_{k \in \mathcal{K}}$; reconfiguration delay δ

Output: flow allocations $\{D_m^k\}_{m \in \mathcal{M}, k \in \mathcal{K}}$ and circuit schedules $\{S_m^k\}_{m \in \mathcal{M}, k \in \mathcal{K}}$ for all cores

```

▷ COFLOW ORDERING
1: Solve the LP relaxation and obtain the optimal solution
    $\{\tilde{T}_m\}_{m \in \mathcal{M}}$ 
2: Sort coflows in non-decreasing order of  $\tilde{T}_m$  and re-index:
    $\tilde{T}_1 \leq \tilde{T}_2 \leq \dots \leq \tilde{T}_M$ 
▷ FLOW ALLOCATION
3: Initialize  $D_{1:0}^k \leftarrow \mathbf{0}_{N \times N}$  for all  $k \in \mathcal{K}$ 
4: for  $m = 1$  to  $M$  do
5:   Initialize  $D_{1:m}^k \leftarrow D_{1:m-1}^k$  for all  $k \in \mathcal{K}$ 
6:   Initialize  $D_m^k \leftarrow \mathbf{0}_{N \times N}$  for all  $k \in \mathcal{K}$ 
7:    $\mathcal{F}_m \triangleq \{f_m(i, j) \mid d_m(i, j) > 0\}$ 
8:   Sort  $\mathcal{F}_m$  in non-increasing order of  $d_m(i, j)$ 
9:   for each flow  $f_m(i, j)$  in  $\mathcal{F}_m$  do
10:     $k^* \leftarrow \operatorname{argmin}_{k \in \mathcal{K}} T_{\text{LB}}^k(D_{1:m}^k \oplus d_m(i, j))$ 
11:    Allocate the entire flow  $f_m(i, j)$  to core  $k^*$ 
12:     $D_m^{k^*} = D_m^{k^*} \oplus d_m(i, j)$ 
13:     $D_{1:m}^{k^*} \leftarrow D_{1:m}^{k^*} \oplus d_m(i, j)$ 
14:   end for
15: end for
▷ CIRCUIT SCHEDULING
16: for each  $k \in \mathcal{K}$  do
17:   for each  $m \in \mathcal{M}$  do
18:     $S_m^k \leftarrow \emptyset$ 
19:   end for
20:    $\mathcal{F}^k \triangleq \bigcup_{m \in \mathcal{M}} \{f_m^k(i, j) \mid d_m^k(i, j) > 0\}$  ▷ processed
   in the re-indexed global order
21:   while  $\mathcal{F}^k \neq \emptyset$  do
22:    for each  $f_m^k(i, j) \in \mathcal{F}^k$  do
23:     if  $f_m^k(i, j)$  is released and both ingress  $i$  and
     egress  $j$  are idle then
24:       $T_m^k(i, j) \leftarrow t_m^k(i, j) + \delta + \frac{d_m^k(i, j)}{r^k}$  ▷
       $t_m^k(i, j) \leftarrow$  earliest feasible time no earlier than  $a_m$ 
25:      Add  $(i, j, t_m^k(i, j))$  to  $S_m^k$ 
26:      Remove  $f_m^k(i, j)$  from  $\mathcal{F}^k$ 
27:     end if
28:    end for
29:   end while
30: end for

```

completion time is given by $T_m^k(i, j) \leftarrow t_m^k(i, j) + \delta + \frac{d_m^k(i, j)}{r^k}$ (Line 24). The scheduled subflow is then recorded in S_m^k (Line 25) and removed from \mathcal{F}^k (Line 26).

C. Analysis of Performance Guarantees

For each coflow C_m and each port $p \in \mathcal{I} \cup \mathcal{J}$, let $\rho_{m,p}$ denote the aggregate traffic load of C_m incident to port p , and let $\tau_{m,p}$ denote the number of nonzero flow entries of

C_m incident to port p . For any prefix set $L_m = \{1, \dots, m\}$, define the prefix-aggregated matrix $D_{1:m} \triangleq \sum_{\ell=1}^m D_\ell$, and for each core k , define $D_{1:m}^k \triangleq \sum_{\ell=1}^m D_\ell^k$.

For any port $p \in \mathcal{I} \cup \mathcal{J}$, let $\rho_{1:m,p}$ and $\tau_{1:m,p}$ denote the aggregate traffic load and the number of nonzero entries incident to port p in $D_{1:m}$, respectively. Let $\rho_{1:m}$ and $\tau_{1:m}$ denote the maximum aggregate traffic load and the maximum number of nonzero entries incident to any port in $D_{1:m}$, respectively. Specifically, define $\rho_{1:m} \triangleq \max_{p \in \mathcal{I} \cup \mathcal{J}} \rho_{1:m,p}$ and $\tau_{1:m} \triangleq \max_{p \in \mathcal{I} \cup \mathcal{J}} \tau_{1:m,p}$. Let $r_{\max} \triangleq \max_{k \in \mathcal{K}} r^k$.

Our proof proceeds in three steps. First, we use the LP constraints to derive prefix-aware global bounds on $\rho_{1:m}$ and $\tau_{1:m}$ in terms of \tilde{T}_m . Second, we show that the greedy inter-core flow allocation transforms these global prefix bounds into a bound on the maximum per-core prefix lower bound $\max_k T_{\text{LB}}^k(D_{1:m}^k)$. Third, we prove that the completion time of coflow C_m under the intra-core circuit scheduling policy is upper bounded by a constant-factor multiple of $\max_k T_{\text{LB}}^k(D_{1:m}^k)$. Combining these three ingredients yields the claimed approximation guarantee.

1) *Derivation of Ordering-Phase Prefix Bound:*

Lemma 2 (Transmission-Capacity Prefix Bound). *For any prefix set $L_m = \{1, \dots, m\}$ and any fixed port $p \in \mathcal{I} \cup \mathcal{J}$, $\sum_{\ell=1}^m \rho_{\ell,p} \tilde{T}_\ell \geq \frac{1}{2R} (\sum_{\ell=1}^m \rho_{\ell,p})^2$. Consequently, $\rho_{1:m} \leq 2R\tilde{T}_m$.*

Proof: The proof follows the similar prefix-based analysis for ordering LP relaxations [15]. We first establish the transmission bound. By the transmission-capacity constraints in Eq. (4), for each $\ell \in L_m$,

$$\tilde{T}_\ell \geq \frac{1}{R} \left(\rho_{\ell,p} + \sum_{q \neq \ell} \rho_{q,p} x_{q,\ell} \right). \quad (7)$$

Multiplying both sides by $\rho_{\ell,p}$ and summing over $\ell = 1, \dots, m$, we obtain

$$\sum_{\ell=1}^m \rho_{\ell,p} \tilde{T}_\ell \geq \frac{1}{R} \left(\sum_{\ell=1}^m \rho_{\ell,p}^2 + \sum_{\ell=1}^m \sum_{\substack{q=1 \\ q \neq \ell}}^m \rho_{\ell,p} \rho_{q,p} x_{q,\ell} \right). \quad (8)$$

Now consider any pair ℓ, q with $1 \leq \ell < q \leq m$. Since the LP imposes $x_{\ell,q} + x_{q,\ell} = 1$, we have $\rho_{\ell,p} \rho_{q,p} x_{q,\ell} + \rho_{q,p} \rho_{\ell,p} x_{\ell,q} = \rho_{\ell,p} \rho_{q,p}$. Therefore,

$$\sum_{\ell=1}^m \sum_{\substack{q=1 \\ q \neq \ell}}^m \rho_{\ell,p} \rho_{q,p} x_{q,\ell} = \sum_{1 \leq \ell < q \leq m} \rho_{\ell,p} \rho_{q,p}. \quad (9)$$

which implies

$$\sum_{\ell=1}^m \rho_{\ell,p} \tilde{T}_\ell \geq \frac{1}{2R} \left(\sum_{\ell=1}^m \rho_{\ell,p} \right)^2. \quad (10)$$

Next, since the LP completion values are ordered non-decreasingly, we have $\tilde{T}_\ell \leq \tilde{T}_m$ for every $\ell \leq m$. Hence,

$$\tilde{T}_m \sum_{\ell=1}^m \rho_{\ell,p} \geq \frac{1}{2R} \left(\sum_{\ell=1}^m \rho_{\ell,p} \right)^2, \quad (11)$$

which implies

$$\sum_{\ell=1}^m \rho_{\ell,p} \leq 2R\tilde{T}_m. \quad (12)$$

Taking the maximum over all $p \in \mathcal{I} \cup \mathcal{J}$ gives

$$\rho_{1:m} \leq 2R\tilde{T}_m. \quad (13)$$

This completes the proof. \blacksquare

Lemma 3 (Reconfiguration-Capacity Prefix Bound). *For any prefix set $L_m = \{1, \dots, m\}$ and any fixed port $p \in \mathcal{I} \cup \mathcal{J}$, $\sum_{\ell=1}^m \tau_{\ell,p} \tilde{T}_\ell \geq \frac{\delta}{2K} (\sum_{\ell=1}^m \tau_{\ell,p})^2$. Consequently, $\tau_{1:m} \leq \frac{2K}{\delta} \tilde{T}_m$.*

Proof: The proof for the reconfiguration bound is analogous. By the reconfiguration-capacity constraints in Eq. (5), for each $\ell \in L_m$,

$$\tilde{T}_\ell \geq \frac{\delta}{K} \left(\tau_{\ell,p} + \sum_{q \neq \ell} \tau_{q,p} x_{q,\ell} \right). \quad (14)$$

Repeating the same argument yields

$$\tau_{1:m} \leq \frac{2K}{\delta} \tilde{T}_m. \quad (15)$$

This completes the proof. \blacksquare

2) *Derivation of Allocation-Phase Prefix Bound:*

Lemma 4 (Allocation-Phase Prefix Bound). *For any $m \in \mathcal{M}$, the prefix-aggregated matrices $\{D_{1:m}^k\}_{k \in \mathcal{K}}$ generated by the allocation phase of Algorithm 1 satisfy $\max_{k \in \mathcal{K}} T_{\text{LB}}^k(D_{1:m}^k) \leq \frac{\rho_{1:m}}{r_{\max}} + \tau_{1:m} \delta$.*

Proof: Consider any non-empty core k_1 after processing the first m coflows. Let $\bar{f}^{k_1}(i, j)$ be the last flow allocated to core k_1 during the allocation of the first m coflows in L_m , and let $\bar{d}^{k_1}(i, j)$ denote its size. Let \bar{D}^{k_1} be the aggregate demand matrix on core k_1 immediately before allocating $\bar{f}^{k_1}(i, j)$. The final aggregate demand on core k_1 is $D_{1:m}^{k_1} = \bar{D}^{k_1} \oplus \bar{d}^{k_1}(i, j)$.

Since Algorithm 1 allocates each flow greedily to the core with the minimum single-core prefix lower bound, when $\bar{f}^{k_1}(i, j)$ was allocated, for any core $k_2 \in \mathcal{K}$,

$$T_{\text{LB}}^{k_1}(\bar{D}^{k_1} \oplus \bar{d}^{k_1}(i, j)) \leq T_{\text{LB}}^{k_2}(\bar{D}^{k_2} \oplus \bar{d}^{k_1}(i, j)), \quad (16)$$

where \bar{D}^{k_2} denotes the aggregate matrix on core k_2 at that time.

By the monotonicity of $T_{\text{LB}}^k(\cdot)$, it follows that

$$T_{\text{LB}}^{k_2}(\bar{D}^{k_2} \oplus \bar{d}^{k_1}(i, j)) \leq T_{\text{LB}}^{k_2}(D_{1:m}). \quad (17)$$

Combining the above inequalities gives, for every $k_2 \in \mathcal{K}$,

$$T_{\text{LB}}^{k_1}(D_{1:m}^{k_1}) \leq T_{\text{LB}}^{k_2}(D_{1:m}), \quad (18)$$

where $T_{\text{LB}}^{k_1}(D_{1:m}^{k_1}) = T_{\text{LB}}^{k_1}(\bar{D}^{k_1} \oplus \bar{d}^{k_1}(i, j))$.

Since this holds for all $k_2 \in \mathcal{K}$, we obtain

$$T_{\text{LB}}^{k_1}(D_{1:m}^{k_1}) \leq \min_{k \in \mathcal{K}} T_{\text{LB}}^k(D_{1:m}). \quad (19)$$

Because k_1 is an arbitrary nonempty core, taking the maximum over all $k \in \mathcal{K}$ gives

$$\max_{k \in \mathcal{K}} T_{\text{LB}}^k (D_{1:m}^k) \leq \min_{k \in \mathcal{K}} T_{\text{LB}}^k (D_{1:m}). \quad (20)$$

Finally, by the definition of $T_{\text{LB}}^k(\cdot)$ (Eq. (1)) applied to the matrix $D_{1:m}$,

$$T_{\text{LB}}^k (D_{1:m}) = \max_{p \in \mathcal{I} \cup \mathcal{J}} L_{1:m,p}^k \leq \frac{\rho_{1:m}^k}{r^k} + \tau_{1:m} \delta, \quad (21)$$

where $L_{1:m,p}^k = \frac{\rho_{1:m,p}^k}{r^k} + \tau_{1:m,p} \delta$.

Taking the minimum over k and using $\min_k \frac{1}{r^k} = \frac{1}{r_{\max}}$, we obtain

$$\max_k T_{\text{LB}}^k (D_{1:m}^k) \leq \min_k \left(\frac{\rho_{1:m}^k}{r^k} + \tau_{1:m} \delta \right) \leq \frac{\rho_{1:m}}{r_{\max}} + \tau_{1:m} \delta. \quad (22)$$

This completes the proof. \blacksquare

3) *Derivation of Scheduling-Phase Prefix Bound:* Let T_m denote the final coflow completion time (CCT) of C_m under Algorithm 1.

Lemma 5 (Scheduling-Phase Prefix Bound). *For any $m \in \mathcal{M}$, the completion time of coflow C_m satisfies $T_m = \max_{k \in \mathcal{K}} T_m^k \leq a_m + 2 \max_{k \in \mathcal{K}} T_{\text{LB}}^k (D_{1:m}^k)$.*

Proof: Fix any core $k \in \mathcal{K}$ such that $D_m^k \neq \mathbf{0}$, i.e., coflow C_m has at least one nonzero flow allocated to core k . Let (i^*, j^*) be the port-pair corresponding to the last completed flow of C_m on core k , and let $d^* = d_m^k(i^*, j^*) > 0$ denote its size. Let $t^* = t_m^k(i^*, j^*)$ be the circuit establishment time of flow $f_m^k(i^*, j^*)$. Since C_m cannot be scheduled before its release time, we have $t^* \geq a_m$.

Under *not-all-stop* reconfiguration, the flow $f_m^k(i^*, j^*)$ starts transmission at time $t^* + \delta$ and completes at

$$T_m^k(i^*, j^*) = t^* + \delta + \frac{d^*}{r^k}. \quad (23)$$

Because (i^*, j^*) corresponds to the last completed flow of C_m on core k , we have

$$T_m^k = \max_{i,j} T_m^k(i, j) = T_m^k(i^*, j^*). \quad (24)$$

Now consider the scheduling policy on core k , which is port-exclusive, non-preemptive, and work-conserving, and respects the global priority order. For any time $t \in [a_m, t^*)$, at least one of the two ports i^* and j^* must be busy; otherwise, the flow $f_m^k(i^*, j^*)$ could have been scheduled earlier, contradicting the definition of t^* .

Let $B_{i^*}(a_m, t^*)$ and $B_{j^*}(a_m, t^*)$ denote the total busy times of ports i^* and j^* over the interval $[a_m, t^*)$, respectively. Define $\rho_{1:m,i^*}^k \triangleq \sum_{j=1}^N d_{1:m}^k(i^*, j)$ as the prefix load incident to port i^* on core k , and define $\tau_{1:m,i^*}^k \triangleq \sum_{j=1}^N \mathbf{1}[d_{1:m}^k(i^*, j) > 0]$ as the number of distinct nonzero port pairs incident to i^* in the prefix matrix $D_{1:m}^k$.

Port i^* can be busy during $[a_m, t^*)$ for two reasons:

(1) *Transmission busy time bound on i^* .* Before the circuit (i^*, j^*) is established, any transmission incident to i^* must correspond to a nonzero entry in the prefix matrix $D_{1:m}^k$,

excluding the transmission of flow $f_m^k(i^*, j^*)$ itself. Hence, the total amount of prefix data that can be transmitted through port i^* before time t^* is at most $\rho_{1:m,i^*}^k - d^*$, and thus the total transmission busy time on i^* is at most $\frac{\rho_{1:m,i^*}^k - d^*}{r^k}$.

(2) *Reconfiguration busy time bound on i^* .* Port i^* is incident to at most $\tau_{1:m,i^*}^k$ distinct nonzero port pairs in $D_{1:m}^k$. Since (i^*, j^*) is the pair established at time t^* , there can be at most $\tau_{1:m,i^*}^k - 1$ circuit establishments involving i^* prior to t^* . Each such establishment incurs a delay δ on the ports involved. Therefore, the total circuit establishment time on i^* before t^* is at most $(\tau_{1:m,i^*}^k - 1) \delta$.

Combining the above two bounds yields

$$B_{i^*}(a_m, t^*) \leq \frac{\rho_{1:m,i^*}^k - d^*}{r^k} + (\tau_{1:m,i^*}^k - 1) \delta. \quad (25)$$

By the same argument for the egress port j^* ,

$$B_{j^*}(a_m, t^*) \leq \frac{\rho_{1:m,j^*}^k - d^*}{r^k} + (\tau_{1:m,j^*}^k - 1) \delta. \quad (26)$$

Since for any time $t \in [a_m, t^*)$ at least one of the two ports i^* and j^* is busy, the interval length is bounded by the sum of their busy times:

$$\begin{aligned} t^* - a_m &\leq B_{i^*}(a_m, t^*) + B_{j^*}(a_m, t^*) \\ &\leq \frac{\rho_{1:m,i^*}^k + \rho_{1:m,j^*}^k - 2d^*}{r^k} + (\tau_{1:m,i^*}^k + \tau_{1:m,j^*}^k - 2) \delta. \end{aligned} \quad (27)$$

Substituting this into $T_m^k = t^* + \delta + \frac{d^*}{r^k}$ gives

$$T_m^k \leq a_m + \frac{\rho_{1:m,i^*}^k + \rho_{1:m,j^*}^k}{r^k} + (\tau_{1:m,i^*}^k + \tau_{1:m,j^*}^k) \delta. \quad (28)$$

By the definition of $T_{\text{LB}}^k(D_{1:m}^k)$, we have

$$\frac{\rho_{1:m,i^*}^k}{r^k} + \tau_{1:m,i^*}^k \delta \leq T_{\text{LB}}^k(D_{1:m}^k), \quad (29)$$

and

$$\frac{\rho_{1:m,j^*}^k}{r^k} + \tau_{1:m,j^*}^k \delta \leq T_{\text{LB}}^k(D_{1:m}^k). \quad (30)$$

Hence,

$$T_m^k \leq a_m + 2T_{\text{LB}}^k(D_{1:m}^k). \quad (31)$$

Finally, taking the maximum over all cores yields

$$T_m = \max_{k \in \mathcal{K}} T_m^k \leq a_m + 2 \max_{k \in \mathcal{K}} T_{\text{LB}}^k(D_{1:m}^k). \quad (32)$$

This completes the proof. \blacksquare

4) *Derivation of Deterministic Approximation Ratio:*

Theorem 1. *Algorithm 1 achieves an $(8K + 1)$ -approximation for minimizing the total weighted CCT in a heterogeneous multi-core OCS network, i.e., $\sum_{m=1}^M w_m T_m \leq (8K + 1) \sum_{m=1}^M w_m T_m^*$, where K is the number of OCS cores.*

Proof: By Lemma 2 and Lemma 3, for any $m \in \mathcal{M}$, the prefix transmission and reconfiguration bottlenecks satisfy $\rho_{1:m} \leq 2R\tilde{T}_m$ and $\tau_{1:m} \leq \frac{2K}{\delta}\tilde{T}_m$. By Lemma 4, we

have $\max_{k \in \mathcal{K}} T_{\text{LB}}^k(D_{1:m}^k) \leq \frac{\rho_{1:m}}{r_{\max}} + \tau_{1:m}\delta$, where $r_{\max} \triangleq \max_{k \in \mathcal{K}} r^k$.

Substituting the above prefix bounds yields

$$\max_{k \in \mathcal{K}} T_{\text{LB}}^k(D_{1:m}^k) \leq \frac{2R\tilde{T}_m}{r_{\max}} + 2K\tilde{T}_m. \quad (33)$$

Since $R = \sum_{k \in \mathcal{K}} r^k \leq Kr_{\max}$, it follows that $\frac{R}{r_{\max}} \leq K$. Therefore,

$$\max_{k \in \mathcal{K}} T_{\text{LB}}^k(D_{1:m}^k) \leq 4K\tilde{T}_m. \quad (34)$$

Furthermore, by Lemma 5, the completion time of coflow C_m under Algorithm 1 satisfies $T_m \leq a_m + 2\max_{k \in \mathcal{K}} T_{\text{LB}}^k(D_{1:m}^k)$. Combining the above inequalities yields

$$T_m \leq a_m + 8K\tilde{T}_m. \quad (35)$$

According to Eq. (6), for each m , we have $\tilde{T}_m \geq a_m$. Hence

$$T_m \leq \tilde{T}_m + 8K\tilde{T}_m \leq (8K + 1)\tilde{T}_m. \quad (36)$$

Multiplying both sides by w_m and summing over all $m \in \mathcal{M}$, we obtain

$$\sum_{m=1}^M w_m T_m \leq (8K + 1) \sum_{m=1}^M w_m \tilde{T}_m. \quad (37)$$

Since the LP objective provides a lower bound on the optimal weighted CCT of the original problem, thus,

$$\sum_{m=1}^M w_m \tilde{T}_m \leq \sum_{m=1}^M w_m T_m^*. \quad (38)$$

Combining the above inequalities gives

$$\sum_{m=1}^M w_m T_m \leq (8K + 1) \sum_{m=1}^M w_m T_m^*. \quad (39)$$

This completes the proof. \blacksquare

Corollary 1. *Algorithm 1 achieves an $8K$ -approximation for minimizing the total weighted CCT when all coflows are released at time zero (i.e., $a_m = 0$) in a heterogeneous multi-core OCS network, i.e., $\sum_{m=1}^M w_m T_m \leq 8K \sum_{m=1}^M w_m T_m^*$, where K is the number of OCS cores.*

Besides multi-core OCS networks, Algorithm 1 can also be naturally applied to multi-core EPS networks by removing the reconfiguration-capacity constraints (Eq. 5) from the LP relaxation and replacing the OCS-specific lower bounds $T_{\text{LB}}^k(\cdot)$ and $T_{\text{LB}}(\cdot)$, and ignoring reconfiguration delay δ (i.e., $\delta = 0$). The overall three-stage algorithm framework remains unchanged: coflows are first ordered globally, then flows are allocated across cores, and finally each core schedules its allocated traffic independently.

Consider an H -core EPS network, where each core $h \in \mathcal{H} = \{1, \dots, H\}$ provides per-port transmission rate r^h . Let $R = \sum_{h \in \mathcal{H}} r^h$ and $r_{\max} = \max_{h \in \mathcal{H}} r^h$. For any demand matrix D_m^h allocated to core h , define the single-core lower bound of EPS as $\bar{T}_{\text{LB}}^h(D_m^h) \triangleq \frac{\rho_m^h}{r^h}$, and define the global EPS lower bound as $\bar{T}_{\text{LB}}(D_m) \triangleq \frac{\rho_m}{R}$ [28]. Let \bar{T}_m^* denote the

completion time of coflow C_m in an optimal schedule for the multi-core EPS network.

Theorem 2. *Algorithm 1 (EPS variant) achieves a $(4H + 1)$ -approximation for minimizing the weighted CCT in a multi-core EPS network, i.e., $\sum_{m=1}^M w_m \bar{T}_m \leq (4H + 1) \sum_{m=1}^M w_m \bar{T}_m^*$.*

Proof: The ordering-phase prefix analysis remains valid with only the transmission-capacity constraints, yielding $\rho_{1:m} \leq 2R\hat{T}_m$, where \hat{T}_m denotes the LP completion value of coflow C_m in the EPS ordering LP. Since reconfiguration is absent, the allocation-phase prefix bound becomes

$$\max_{h \in \mathcal{H}} \bar{T}_{\text{LB}}^h(D_{1:m}^h) \leq \frac{\rho_{1:m}}{r_{\max}}. \quad (40)$$

Following the same prefix-based analysis, the completion time of coflow C_m in the EPS setting satisfies

$$\begin{aligned} \bar{T}_m &\leq a_m + 2 \max_{h \in \mathcal{H}} \bar{T}_{\text{LB}}^h(D_{1:m}^h) \leq a_m + 2 \frac{\rho_{1:m}}{r_{\max}} \\ &= a_m + 4 \frac{R\hat{T}_m}{r_{\max}} \leq a_m + 4H\hat{T}_m. \end{aligned} \quad (41)$$

Finally, we can get

$$\sum_{m=1}^M w_m \bar{T}_m \leq (4H + 1) \sum_{m=1}^M w_m \bar{T}_m^*. \quad (42)$$

This completes the proof. \blacksquare

Corollary 2. *Algorithm 1 (EPS variant) achieves a $4H$ -approximation for minimizing the total weighted CCT when all coflows are released at time zero (i.e., $a_m = 0$) in a heterogeneous multi-core EPS network, i.e., $\sum_{m=1}^M w_m \bar{T}_m \leq 4H \sum_{m=1}^M w_m \bar{T}_m^*$, where H is the number of EPS cores.*

V. EXPERIMENTAL EVALUATIONS

In this section, we evaluate the performance of the proposed Algorithm 1 through trace-driven simulations based on a realistic Facebook workload.

A. Experimental Setup

This subsection describes the workload, evaluation metrics, and default parameter settings.

Workload: We employ the widely adopted Facebook trace [38], collected from a MapReduce cluster consisting of 3000 machines and 150 racks. This data trace has been extensively used in prior coflow scheduling studies [12], [13], [19], [20], [22], [24], [28]. It contains 526 coflows and is commonly reduced to a 150-port network while preserving the original inter-arrival characteristics. For each coflow, the trace provides receiver-level information, including the set of receivers, the traffic received by each receiver, and the corresponding sender, rather than explicit flow-level demands. To construct the $N \times N$ demand matrix for each coflow, we transform the receiver-level traffic into sender-receiver flows. Specifically, for each receiver, the total received traffic is distributed pseudo-uniformly among its associated senders, introducing a small random

perturbation to avoid perfectly uniform splitting. Finally, N machines are randomly selected from the trace as servers and mapped to ingress and egress ports, yielding an N -port coflow instance.

Performance Metrics: Our primary optimization objective is to minimize the total weighted coflow completion time (CCT), given by $\sum_{m=1}^M w_m T_m$. We evaluate all schemes using the normalized total weighted CCT, defined as

$$\text{NormW}(\mathcal{A}) \triangleq \frac{\sum_{m=1}^M w_m T_m(\mathcal{A})}{\sum_{m=1}^M w_m T_m(\text{OURS})},$$

where OURS denotes Algorithm 1. By definition, $\text{NormW}(\text{OURS}) = 1$, and a larger value indicates worse performance relative to OURS. In addition, we also report tail CCT statistics, specifically p95 and p99 CCT. These metrics capture the latency experienced by the most delayed coflows and are particularly useful for reflecting the impact of inter-core contention, port conflicts, and reconfiguration overhead on long-tail performance.

Finally, to quantify the gap between practical performance and the theoretical worst-case guarantee, we report the approximation ratio of OURS, defined as

$$\text{Approx} \triangleq \frac{\sum_{m=1}^M w_m T_m(\text{OURS})}{\sum_{m=1}^M w_m \tilde{T}_m(LP)},$$

where $\tilde{T}_m(LP)$ denotes the objective value of the LP relaxation.

Default Parameters. Unless stated otherwise, we adopt the following default parameters: (i) number of ports $N = 10$; (ii) number of coflows $M = 100$ (randomly sampled from the trace); (iii) number of cores $K = 3$; (iv) core rate vector $[10, 20, 30]$; (v) aggregated port rate $R = 60$; and (vi) reconfiguration delay $\delta = 8$.

B. Baseline Solutions

To the best of our knowledge, there is currently no prior scheduler specifically designed for multi-coflow scheduling in multi-core OCS networks under the *not-all-stop* reconfiguration model. We therefore construct representative baselines by replacing or ablating individual components of Algorithm 1 (OURS).

- **WSPT-ORDER** Following prior work [31], considering a heuristic global coflow ordering rule in place of the LP-guided ordering of Algorithm 1. Specifically, each coflow C_m is assigned a priority score $w_m/T_{LB}(D_m)$, where $T_{LB}(D_m) = \delta + \frac{\rho_m}{R}$. Coflows are subsequently sorted in non-increasing order based on this score. This ordering rule prioritizes coflows with higher weights and lower intrinsic service requirements, thereby approximating the weighted shortest-processing-time (WSPT) principle. The inter-core flow allocation and intra-core circuit scheduling procedures remain unchanged from those in Algorithm 1.
- **SUNFLOW-S** Replace the intra-core circuit scheduling module in Algorithm 1 with Sunflow [20] under the *not-all-stop* model. The global coflow order and inter-core flow allocation remain unchanged.

- **BvN-S** Replace the intra-core circuit scheduling module in Algorithm 1 with Birkhoff-von Neumann (BvN) decomposition [36] under the *all-stop* model. Since BvN decomposition applies to doubly stochastic matrices, the demand matrix must first be transformed into a doubly stochastic form before decomposition is performed. The global coflow order and inter-core flow allocation remain unchanged.
- **LOAD-ONLY** Replace the τ -aware inter-core flow allocation in Algorithm 1 with a load-only policy. Each flow is assigned to the core that minimizes $\rho_{1:m}^k/r^k$, i.e., the reconfiguration term $\tau_{1:m}^k \delta$ is ignored. The global coflow order and intra-core circuit scheduling remain unchanged.

C. Experimental Results

We first evaluate the performance of Algorithm 1 under the default setting. We then vary the reconfiguration delay δ and the number of ports N to examine how performance changes. To cover different multi-core network configurations, we consider $K = 3, 4, 5$ under both imbalanced-rate and balanced-rate settings. Finally, we report the approximation ratios for different values of δ .

1) *Performance under the Default Setting:* Fig. 3 reports the normalized total weighted CCT and normalized tail CCT (p95/p99) under the default setting, with all results normalized to OURS. LOAD-ONLY increases the normalized total weighted CCT to $1.37\times$, while the normalized p95 and p99 tail CCT rise to $1.33\times$ and $1.32\times$, respectively. This confirms that ignoring reconfiguration overhead during inter-core allocation leads to inferior flow placements. Replacing the intra-core scheduler with Sunflow (SUNFLOW-S) yields a similar increase in total weighted CCT ($1.38\times$), but causes much more severe tail degradation, with p95 and p99 reaching $2.22\times$ and $2.26\times$. BvN-S performs the worst, reaching $4.34\times$ normalized total weighted CCT, $6.89\times$ normalized p95, and $7.07\times$ normalized p99.

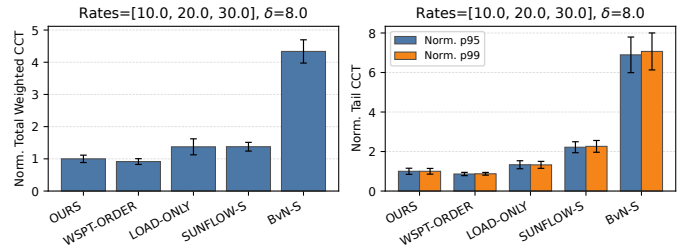


Fig. 3: Normalized Total Weighted CCT and Tail CCT (p95/p99) under the Default Setting.

Notably, WSPT-ORDER slightly outperforms OURS, achieving $0.92\times$ normalized total weighted CCT. This result is consistent with common workload characteristics in data center networks, where coflow sizes are typically heavy-tailed and flow sizes within each coflow can be highly skewed. In such cases, efficient completion behavior is typically dominated by a small number of large flows, making WSPT-based

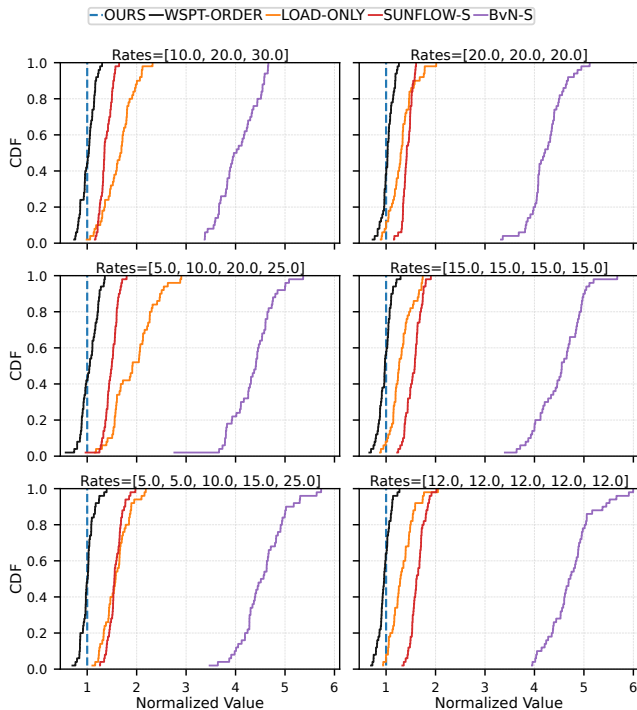


Fig. 4: CDF of Normalized Weighted CCT for $K = 3, 4, 5$.

ordering highly competitive in practice. This observation does not contradict our theoretical results. Our LP-guided ordering method is primarily designed to support the approximation analysis and establish provable worst-case guarantees, whereas the WSPT-based priority rule may better match the structure of these real-world workloads, thereby yielding a slightly lower empirically weighted CCT.

2) *Performance Evaluation*: To further examine the stability of the relative performance, Fig. 4 presents the CDF of the normalized total weighted CCT under imbalanced and balanced rate settings for $K = 3, 4, 5$.

3) *Impact of Reconfiguration Delay (δ -Sensitivity)*: Table III evaluates the impact of reconfiguration delay $\delta = 2, 4, 6, 8, 10, 12$ on final performance for $K = 3, 4, 5$, under both imbalanced and balanced rate settings. Among the baselines, WSPT-ORDER performs closest to OURS, and in some cases even achieves values slightly below 1. In contrast, LOAD-ONLY consistently performs worse, especially under imbalanced-rate settings, confirming that ignoring reconfiguration overhead during inter-core allocation leads to inferior flow placements. BvN-S exhibits the largest performance gap, with its normalized total weighted CCT typically ranging from approximately $3.6\times$ to $5.2\times$.

4) *Impact of the Number of Ports (N -Scaling)*: Fig. 5 illustrates the normalized total weighted CCT as the number of ports varies over $N \in \{8, 12, 16, 24, 32\}$, with $M = 100$ and $\delta = 8$. Overall, across all settings, OURS consistently outperforms LOAD-ONLY, SUNFLOW-S, and BvN-S, while WSPT-ORDER remains the strongest baseline and stays close to OURS. Furthermore, as the number of cores increases, the

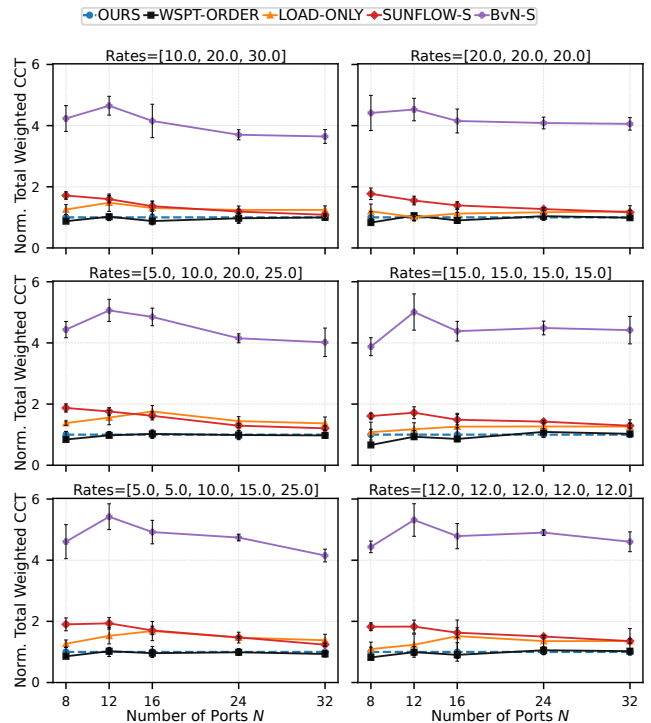


Fig. 5: Normalized Total Weighted CCT versus Number of Ports N for $K = 3, 4, 5$.

advantage of our method over LOAD-ONLY, SUNFLOW-S, and BvN-S becomes more significant.

5) *Approximation Ratio versus Reconfiguration Delay*: Fig. 6 shows the approximation ratio of OURS under different reconfiguration delay δ values, for both zero-release and arbitrary-release settings. Two observations are immediately evident. First, the observed approximation ratios are consistently much lower than the proven worst-case guarantees of $8K$ and $8K + 1$. Across all test configurations, the approximation ratios remain within a much narrower range, mostly between 2.5 and 5.0, rather than approaching the corresponding theoretical bounds. This indicates that the approximation guarantees are conservative, primarily providing robustness in the worst case, while the proposed algorithm performs significantly better in practice on representative instances. Second, the approximation ratio under zero-release time is consistently lower than that under arbitrary-release time. This is expected, as introducing release times adds additional time constraints, making the scheduling problem more challenging.

VI. CONCLUSIONS

This paper investigates the multi-coflow scheduling problem in multi-core data center networks, focusing particularly on multiple OCS cores operating in parallel under the *not-all-stop* (asynchronous) reconfiguration model. In this scenario, the scheduler must jointly account for (i) the coupled capacity constraints across heterogeneous OCS cores due to inter-core traffic allocation and (ii) the intra-core feasibility constraints

TABLE III: Normalized Total Weighted CCT versus Reconfiguration Delay δ for $K = 3, 4, 5$.

δ	WSPT	LOAD	SUN	BvN	δ	WSPT	LOAD	SUN	BvN	δ	WSPT	LOAD	SUN	BvN
Imbalanced rates: [10, 20, 30]					Imbalanced rates: [5, 10, 20, 25]					Imbalanced rates: [5, 5, 10, 15, 25]				
2	1.0433	1.3067	1.4525	3.7783	2	1.0289	1.1777	1.4508	3.6356	2	0.9113	1.0732	1.5024	3.6627
4	1.0222	1.4272	1.4257	4.0436	4	0.9744	1.4584	1.5451	4.2780	4	0.9831	1.3271	1.6377	4.3848
6	0.9221	1.4343	1.3453	4.0609	6	0.9720	1.4905	1.5090	4.4032	6	0.9834	1.3387	1.5864	4.7461
8	0.9156	1.3734	1.3767	4.3356	8	0.9683	1.5270	1.4803	4.4713	8	0.9553	1.4922	1.5969	4.8355
10	0.9938	1.4895	1.4334	4.4845	10	0.9460	1.4413	1.4787	4.5854	10	0.9671	1.5511	1.5683	4.8308
12	0.9259	1.5980	1.3290	4.3408	12	0.9542	1.6088	1.4203	4.4858	12	0.9917	1.5567	1.6362	5.1677
Balanced rates: [20, 20, 20]					Balanced rates: [15, 15, 15, 15]					Balanced rates: [12, 12, 12, 12, 12]				
2	0.9947	1.1150	1.5056	3.8005	2	1.0014	1.2248	1.4542	3.6922	2	1.0741	1.0858	1.4734	3.6548
4	0.9722	1.0824	1.3479	3.8702	4	0.9793	1.2630	1.5781	4.3146	4	0.9431	1.2338	1.6177	4.4731
6	0.9512	1.1293	1.3904	4.1295	6	0.9558	1.3127	1.5298	4.4905	6	0.9798	1.2338	1.5875	4.7659
8	0.9965	1.2076	1.4087	4.3552	8	0.8771	1.3644	1.4022	4.3379	8	0.9393	1.4397	1.5784	4.8658
10	0.9544	1.1736	1.4047	4.3997	10	0.9843	1.5260	1.5788	4.8410	10	0.8742	1.4383	1.4913	4.7138
12	0.9639	1.2806	1.3850	4.4360	12	0.9488	1.5116	1.5195	4.8772	12	0.8310	1.4200	1.5154	4.7411

(a) $K = 3$

(b) $K = 4$

(c) $K = 5$

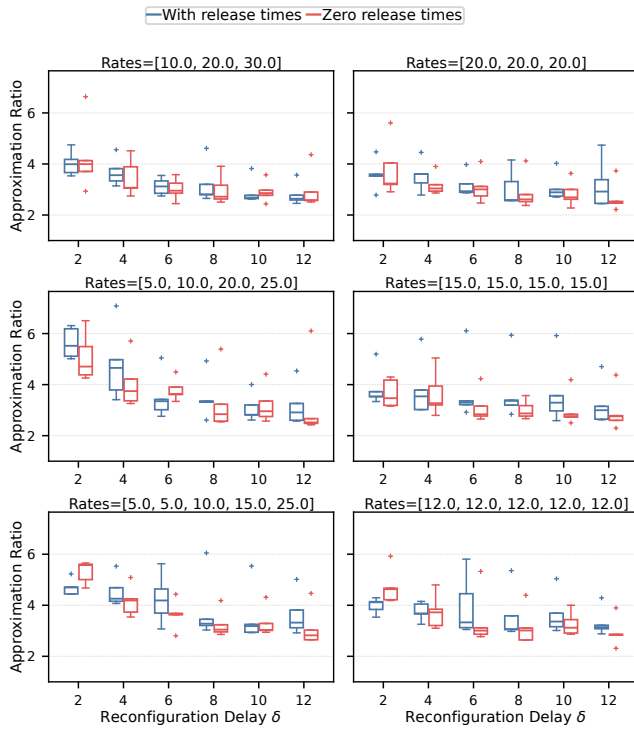


Fig. 6: Approximation Ratio versus Reconfiguration Delay δ for $K = 3, 4, 5$.

induced by port exclusivity and asynchronous reconfiguration delay.

We develop an approximation algorithm for minimizing the total weighted coflow completion time (CCT) and establish a global worst-case performance guarantee. Specifically, in a heterogeneous K -core OCS network, the algorithm achieves an $(8K + 1)$ -approximation for arbitrary release times, and an $8K$ -approximation when all coflows are released at time zero. These guarantees explicitly capture the impact of core parallelism on the scheduling complexity and provide the provable approximation bounds for multi-coflow scheduling in

multi-core OCS networks under asynchronous reconfiguration. We further show that the same algorithm framework can be naturally applied to H -core EPS networks by replacing the OCS-specific lower bounds and setting the reconfiguration delay to zero. In that setting, the resulting EPS variant achieves a $(4H + 1)$ -approximation for arbitrary release times, and a $4H$ -approximation when all coflows are released at time zero.

A promising direction for future research is online scheduling in multi-core OCS networks, where coflows arrive dynamically, and their demand matrices may be only partially observed. The main objective is to develop online algorithms with provable competitive ratios, thereby establishing theoretical foundations for the design of practical system policies.

ACKNOWLEDGEMENT

This work is supported by Department of Environment, Science and Innovation of Queensland State Government under Quantum 2032 Challenge Program (Project #Q2032001) and Key-Area Research and Development Plan of Guangdong Province #2020B010164003. The corresponding author is Hong Shen.

REFERENCES

- [1] J. Dean and S. Ghemawat, "Mapreduce: simplified data processing on large clusters," *Communications of the ACM*, vol. 51, no. 1, pp. 107–113, 2008.
- [2] M. Zaharia, M. Chowdhury, T. Das, A. Dave, J. Ma, M. McCauly, M. J. Franklin, S. Shenker, and I. Stoica, "Resilient distributed datasets: A fault-tolerant abstraction for in-memory cluster computing," in *9th {USENIX} Symposium on Networked Systems Design and Implementation ({NSDI} 12)*, 2012, pp. 15–28.
- [3] M. Isard, M. Buidu, Y. Yu, A. Birrell, and D. Fetterly, "Dryad: distributed data-parallel programs from sequential building blocks," in *Proceedings of the 2nd ACM SIGOPS/EuroSys European Conference on Computer Systems 2007*, 2007, pp. 59–72.
- [4] M. Chowdhury and I. Stoica, "Coflow: A networking abstraction for cluster applications," in *Proceedings of the 11th ACM Workshop on Hot Topics in Networks*, 2012, pp. 31–36.
- [5] M. Chowdhury, M. Zaharia, J. Ma, M. I. Jordan, and I. Stoica, "Managing data transfers in computer clusters with orchestra," *ACM SIGCOMM Computer Communication Review*, vol. 41, no. 4, pp. 98–109, 2011.
- [6] M. Shafiee and J. Ghaderi, "Scheduling coflows with dependency graph," *IEEE/ACM Transactions on Networking*, vol. 30, no. 1, pp. 450–463, 2021.

- [7] M. Chowdhury, Y. Zhong, and I. Stoica, "Efficient coflow scheduling with varys," in *Proceedings of the 2014 ACM conference on SIGCOMM*, 2014, pp. 443–454.
- [8] F. R. Dogar, T. Karagiannis, H. Ballani, and A. Rowstron, "Decentralized task-aware scheduling for data center networks," *ACM SIGCOMM Computer Communication Review*, vol. 44, no. 4, pp. 431–442, 2014.
- [9] S. Luo, H. Yu, Y. Zhao, B. Wu, S. Wang *et al.*, "Minimizing average coflow completion time with decentralized scheduling," in *2015 IEEE International Conference on Communications (ICC)*. IEEE, 2015, pp. 307–312.
- [10] M. Chowdhury and I. Stoica, "Efficient coflow scheduling without prior knowledge," *ACM SIGCOMM Computer Communication Review*, vol. 45, no. 4, pp. 393–406, 2015.
- [11] H. Zhang, L. Chen, B. Yi, K. Chen, M. Chowdhury, and Y. Geng, "Coda: Toward automatically identifying and scheduling coflows in the dark," in *Proceedings of the 2016 ACM SIGCOMM Conference*, 2016, pp. 160–173.
- [12] X. Wang and H. Shen, "Online scheduling of coflows by attention-empowered scalable deep reinforcement learning," *Future Generation Computer Systems*, vol. 146, pp. 195–206, 2023.
- [13] X. Wang, H. Shen, and H. Tian, "Efficient and fair: Information-agnostic online coflow scheduling by combining limited multiplexing with drl," *IEEE Transactions on Network and Service Management*, vol. 20, no. 4, pp. 4572–4584, 2023.
- [14] Z. Qiu, C. Stein, and Y. Zhong, "Minimizing the total weighted completion time of coflows in datacenter networks," in *Proceedings of the 27th ACM symposium on Parallelism in Algorithms and Architectures*, 2015, pp. 294–303.
- [15] M. Shafiee and J. Ghaderi, "An improved bound for minimizing the total weighted completion time of coflows in datacenters," *IEEE/ACM Transactions on Networking*, vol. 26, no. 4, pp. 1674–1687, 2018.
- [16] Z. Wang, H. Zhang, X. Shi, X. Yin, Y. Li, H. Geng, Q. Wu, and J. Liu, "Efficient scheduling of weighted coflows in data centers," *IEEE Transactions on Parallel and Distributed Systems*, vol. 30, no. 9, pp. 2003–2017, 2019.
- [17] C. Xu, H. Tan, J. Hou, C. Zhang, and X.-Y. Li, "Omco: Online multiple coflow scheduling in optical circuit switch," in *2018 IEEE International Conference on Communications (ICC)*. IEEE, 2018, pp. 1–6.
- [18] C. Zhang, H. Tan, C. Xu, X.-Y. Li, S. Tang, and Y. Li, "Reco: Efficient regularization-based coflow scheduling in optical circuit switches," in *2019 IEEE 39th International Conference on Distributed Computing Systems (ICDCS)*. IEEE, 2019, pp. 111–121.
- [19] H. Tan, C. Zhang, C. Xu, Y. Li, Z. Han, and X.-Y. Li, "Regularization-based coflow scheduling in optical circuit switches," *IEEE/ACM Transactions on Networking*, vol. 29, no. 3, pp. 1280–1293, 2021.
- [20] X. S. Huang, X. S. Sun, and T. E. Ng, "Sunflow: Efficient optical circuit scheduling for coflows," in *Proceedings of the 12th International on Conference on emerging Networking EXperiments and Technologies*, 2016, pp. 297–311.
- [21] T. Zhang, F. Ren, J. Bao, R. Shu, and W. Cheng, "Minimizing coflow completion time in optical circuit switched networks," *IEEE Transactions on Parallel and Distributed Systems*, vol. 32, no. 2, pp. 457–469, 2020.
- [22] X. Wang, H. Shen, and H. Tian, "Scheduling coflows in hybrid optical-circuit and electrical-packet switches with performance guarantee," *IEEE/ACM Transactions on Networking*, vol. 32, no. 3, pp. 2299–2314, 2024.
- [23] Z. Li and H. Shen, "Co-scheduler: Accelerating data-parallel jobs in datacenter networks with optical circuit switching," in *2019 IEEE 39th International Conference on Distributed Computing Systems (ICDCS)*. IEEE, 2019, pp. 186–195.
- [24] X. Wang, H. Shen, and H. Tian, "Optimal partitioning of traffic demand for coflow scheduling in hybrid switches," *IEEE Transactions on Network and Service Management*, 2025.
- [25] R. Jiang, T. Zhang, and C. Yi, "Effective coflow scheduling in hybrid circuit and packet switching networks," in *2023 IEEE Symposium on Computers and Communications (ISCC)*. IEEE, 2023, pp. 1156–1161.
- [26] Cisco White Paper. (2016), "The future is 40 gigabit ethernet," <https://www.cisco.com/c/dam/en/us/products/collateral/switches/catalyst-6500-series-switches/white-paper-c11-737238.pdf>.
- [27] Cisco. (2016), "Cisco global cloud index: Forecast and methodology, 2015–2020," <https://www.cisco.com/c/dam/en/us/solutions/collateral/service-provider/global-cloud-index-gci/white-paper-c11-738085.pdf>.
- [28] X. S. Huang, Y. Xia, and T. E. Ng, "Weaver: Efficient coflow scheduling in heterogeneous parallel networks," in *2020 IEEE International Parallel and Distributed Processing Symposium (IPDPS)*. IEEE, 2020, pp. 1071–1081.
- [29] C.-Y. Chen, "Efficient approximation algorithms for scheduling coflows with total weighted completion time in identical parallel networks," *IEEE Transactions on Cloud Computing*, vol. 12, no. 1, pp. 116–129, 2023.
- [30] L. Poutievski, O. Mashayekhi, J. Ong, A. Singh, M. Tariq, R. Wang, J. Zhang, V. Beauregard, P. Conner, S. Gribble *et al.*, "Jupiter evolving: transforming google's datacenter network via optical circuit switches and software-defined networking," in *Proceedings of the ACM SIGCOMM 2022 Conference*, 2022, pp. 66–85.
- [31] X. Wang, H. Shen, H. Tian, and D. Wang, "Scheduling coflows in multi-core ocs networks with performance guarantee," *arXiv preprint arXiv:2604.08242*, 2026. [Online]. Available: <https://doi.org/10.48550/arXiv.2604.08242>
- [32] S. Khuller and M. Purohit, "Brief announcement: Improved approximation algorithms for scheduling co-flows," in *Proceedings of the 28th ACM Symposium on Parallelism in Algorithms and Architectures*, 2016, pp. 239–240.
- [33] C.-Y. Chen, "Scheduling coflows for minimizing the total weighted completion time in heterogeneous parallel networks," *Journal of Parallel and Distributed Computing*, vol. 182, p. 104752, 2023.
- [34] L. Wang and W. Wang, "Fair coflow scheduling without prior knowledge," in *2018 IEEE 38th International Conference on Distributed Computing Systems (ICDCS)*. IEEE, 2018, pp. 22–32.
- [35] B. Tian, C. Tian, B. Wang, B. Li, Z. He, H. Dai, K. Liu, W. Dou, and G. Chen, "Scheduling dependent coflows to minimize the total weighted job completion time in datacenters," *Computer Networks*, vol. 158, pp. 193–205, 2019.
- [36] G. Birkhoff, "Tres observaciones sobre el algebra lineal," *Univ. Nac. Tucuman, Ser. A*, vol. 5, pp. 147–154, 1946.
- [37] T. Gonzalez and S. Sahni, "Open shop scheduling to minimize finish time," *Journal of the ACM (JACM)*, vol. 23, no. 4, pp. 665–679, 1976.
- [38] "Facebooktrace," <https://github.com/coflow/coflow-benchmark>, 2019.